Conference Paper, Published Version

Li, Kanyu; Cao, Zhixian

Computational Study of Roll Waves in Shallow Flow over Erodible Bed

COMPUTATIONAL STUDY OF ROLL WAVES IN SHALLOW FLOW OVER ERODIBLE BED

Kanyu Li[1], Zhixian Cao[2]

[1] Research assistant, State Key Laboratory of Water Resources and Hydropower Engineering Science, Wuhan University, Wuhan, 430072, China.
[2] Corresponding author, Professor, State Key Laboratory of Water Resources and Hydropower Engineering Science, Wuhan University, Wuhan, 430072, China. E-mail: zxcao@whu.edu.cn.

ABSTRACT

A computational study is presented on erodible-bed hydraulics of roll waves with sediment transport and morphological evolution. The governing equations of the model comprise the shallow water hydrodynamics equations closed with the Manning formulation for the boundary resistance. The second-order Total-Variation-Diminishing version of the Weighted-Average-Flux method, along with the HLLC approximate Reimann Solver, is used to solve the governing equations, which can properly represent shock waves. The model is applied to resolve the roll waves in Brock's experiments in a fixed bed channel. Numerical simulations are performed to resolve the evolution of roll waves over erodible bed. The results show that the morphological evolution considerably affects the dynamic characteristics of roll waves, as the infiltration. It is therefore essential to incorporate sediment transport and morphological changes in mathematical modeling of overland flows featuring roll waves in semi-arid and arid areas.

Keywords: roll waves, mobile bed, numerical simulation, infiltration, Froude number

1. INTRODUCTION

It is well known that a steady discharge in a constant slope channel will not always result in a steady uniform flow. If the channel is sufficiently steep and long, the depth of the flow will not remain at its normal value over the entire length of the channel as might be expected. A series of shallow water waves will develop in some reach of the channel and eventually break forming bores that propagate downstream, and may overtake one another when the flow surface is not flat and its longitudinal profile undulates periodically. The series of shallow water waves that develop spontaneously in an overland flow are called roll wave trains. On the basis of limited observations, Cornish (1934) conjectured that roll waves depended primarily on flow resistance and that they would not be formed if there were no resistance. Based on the flow resistance, Thomas (1937) analyzed roll waves and derived a necessary condition for roll waves' formation. Dressler (1949) mathematically reported that the necessary condition for roll wave formation was that the flow resistance was under a certain critical value. On the basis of Dressler's work, Brock (1969) even measured the spontaneously developed roll wave trains in a laboratory channel. He divided the process of roll-wave developing into three phases: (1) the initial developing phase, in which the waves do not overtake or combine with each other; (2) the overtaking phase, in which one shock wave overtakes and combines with other shock waves; and (3) the final developed phase, in which the wave cycle increases with distance as a result of wave overtaking. Zanutigh and Lamberti (2002) numerically simulated roll waves down an inclined rectangular channel under the same conditions as tested by Brock (1969). More analyses on roll waves have been carried out (Liu *et al* 2007; Balmforth and Mandre 2004).

In recent years, the frequent rainfall-induced flash flooding disasters in many mountainous areas have become a significant threat to local population and economy. Overland flow is often seen during the generation phase of flash floods, and roll waves are prone to occur in shallow overland flows. Therefore, enhanced understanding of roll waves will help predict flash flood generation and thus its propagation. However, previous studies on roll waves have been limited to those over fixed bed, and the need for investigations of roll waves over erodible bed is evident, especially when flash flooding generation and propagation in semi-arid and arid areas (e.g., in north-west China) are to be predicted with improved reliability.

This paper presents a computational study on mobile bed hydraulics of roll waves and the induced sediment transport. The governing equations of the model comprise the shallow water hydrodynamics equations closed with Manning roughness for boundary resistance. The second-order Total-Variation-Diminishing version of the Weighted-Average-Flux method, along with the HLLC approximate Reimann Solver, is used to solve the governing equations, which can properly represent shock waves. It is applied to reproduce Brock's experiments (1969) on roll waves in a fixed-bed channel. Numerical simulations are made to illustrate the development of roll waves over mobile bed. The results indicate that the morphological evolution influences the roll waves' dynamic characteristics greatly, as the infiltration.

2. MODEL FORMULATION

2.1 Governing equations

Consider one-dimensional (1D) flow in a channel with rectangular cross sections of constant width and a mobile bed that is composed of uniform and non-cohesive sediment with particle diameter *d*. As infiltration and surface tension are incorporated, the governing equations can be written in conservative form, as an extension of those in Cao *et al*. (2004).

$$\frac{\partial \mathrm{U}}{\partial t}+\frac{\partial \mathrm{F}}{\partial x}=\mathrm{S} \tag{1}$$

where

$$\mathbf{U}=\begin{bmatrix} h \\ hu \\ hc \end{bmatrix}, \quad \mathbf{F}=\begin{bmatrix} hu \\ hu^2+gh^2/2 \\ huc \end{bmatrix} \tag{2a, b}$$

$$\mathbf{S}=\begin{bmatrix} (E-D)/(1-p)-f \\ -gh(\dfrac{\partial z}{\partial x}+S_f)-p_x-\dfrac{(\rho_s-\rho_w)gh^2}{2\rho}\dfrac{\partial c}{\partial x}-\dfrac{(\rho_0-\rho)(E-D)u}{\rho(1-p)} \\ E-D \end{bmatrix} \tag{2c}$$

$$\frac{\partial z}{\partial t}=\frac{D-E}{1-p} \tag{3}$$

where t = time, x = stream wise coordinate, h = flow depth, u = depth-averaged velocity, c = sediment concentration, z = bed elevation, g = gravitational acceleration, ρ_w, ρ_s = densities of water and sediment respectively, $\rho = \rho_w(1-c) + \rho_s$ = density of the mixture, $\rho_0 = \rho_w p + \rho_s(1-p)$ = density of the saturated bed, E, D = sediment entrainment and deposition fluxes, p = bed sediment porosity, $P_x = \sigma / R$ = surface tension, σ = coefficient of capillary, R = radius of curvature; f = infiltration rate.

2.2 Empirical closure relationships

The friction slope S_f is computed using Chézy coefficient C

$$S_f = \frac{u^2}{C^2 R} \tag{4}$$

The determination of the deposition flux according to Richardson and Zaki (1954) is introduced

$$D = w(1-c_a)^m c_a \tag{5}$$

where w= settling velocity of a single particle in tranquil water, c_a = local near-bed sediment concentration in volume, $m = 4.45R^{-0.1}$ = exponent, $R \equiv \sqrt{sgd}d / \nu$, ν = kinematic viscosity, and $s = \rho_s / \rho_w - 1$

The entrainment flux E in overland flow is estimated using the formulation of Sander *et al*. (2007)

$$E = \frac{\psi}{gh\rho_s}(\frac{\rho_s}{\rho_s - \rho_w})(\Omega - \Omega_{cr}) \tag{6}$$

where $\Omega = \rho g s_0 q$, $\Omega_{cr} = 0.007$. Since the research on the entrainment fluxes in overland flow is not completely enough, different coefficients are used to amend the entrainment fluxes. The coefficient ψ is introduced for ascertaining the impacts of entrainment and morphological evolution.

2.3 Numerical algorithm

The numerical algorithm used in the present study is essential the same as in Cao et al. (2004). Briefly, Eq. (1) discretized into

$$\mathbf{U}_i^{k+1} = \mathbf{U}_i^k - \frac{\Delta t}{\Delta x}(\mathbf{F}_{i+1/2} - \mathbf{F}_{i-1/2}) + \Delta t S^k \tag{7}$$

where Δt = time step; Δx = spatial step; I = spatial node index; k = time step index; and $\mathbf{F}_{i+1/2}$ = numerical flux at $x = x_{i+1/2}$, which is computed using second-order TVD version of the Weighted-Average-Flux method, along with the HLLC approximate Reimann Solver (Toro 2001). The bed evolution can be computed by solving Eq. (3),

$$z_i^{k+1} = z_i^k + \Delta t \frac{(D-E)_i^k}{1-p} \tag{8}$$

3. TEST OF MODEL FOR SHALLOW FLOW OVER FIXED BED

3.1 Threshold of instability

In a similar condition to Zanuttigh and Lamberti (2002), a 500 *m* long rectangular channel is considered in the analysis; the value of *C* is imposed at 50.0, remaining constant along the channel; wave period ω is equals to 40 *s,* and the evolution of the periodic perturbation $h' = h(1 + 0.005 \sin \omega t)$ is imposed on upstream (x = 0 *m*) over a uniform flow depth h = 1 m. This section aims to address the threshold of shallow flow instability. As for the value of Froude number (*Fr*), there is no uniform standard so far. According to previous predictions for rectangular channels, the critical value of *Fr* is 2.0; perturbations are attenuated along the channel when *Fr* is lower than 2.0 and are amplified when it is higher than 2.0. Here the water flow is characterized by three different values of *Fr* (0.5, 2.0 and 3.0), and the corresponding bed slopes are: 0.00098, 0.0157 and 0.0353. The computed flow depth profiles at downstream (x = 1000 m) are presented in Figure 1. As is expected, perturbations are attenuated along the channel when *Fr* = 0.5, remaining constant when *Fr* = 2.0, and are amplified when *Fr* = 3.0. As is illustrated from the graph, the threshold appears to be *Fr* = 2.0, which is consistent with the condition of flow threshold formation. Thus, the present 1D model is of reasonable accuracy and reliability, and can be utilized to analyze the formation and evolution of roll waves.

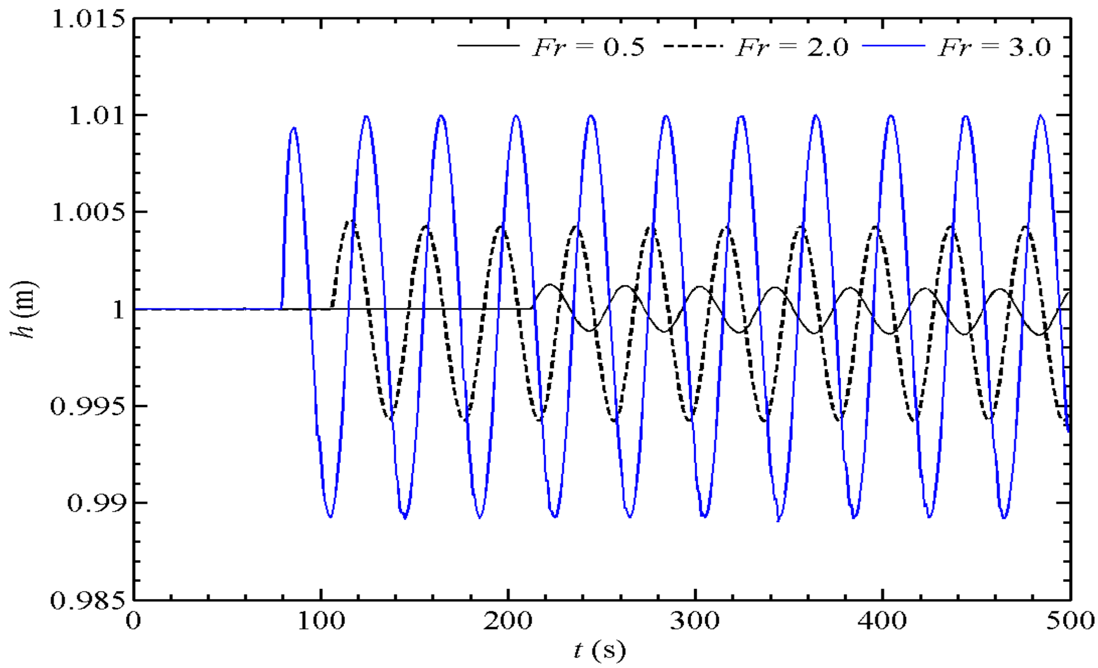

Figure 1. Flow depth *h* versus time *t* at downstream (*x* = 1000 m) for different Froude numbers at inlet (*x* = 0 m)

3.2 Roll waves over fixed bed

Numerical simulations were performed under the same conditions reproduced in Brock's experiments (1969), in which the developing of natural roll waves in an inclined rectangular channel was described, fed by a steady water discharge. At the channel inlet (x = 0 m), a periodic perturbation $h' = h(1 + 0.005\sin\omega t)$ is imposed over a uniform flow depth (h = 0.00797 m), with slope of 0.05011. Manning's equation is used to compute friction slope, with a friction coefficient calculated from C (=55.23) and Fr (=3.71).

Figure 2 shows the evolution process of flow depth h versus time t at two separate sections, where the distance from the channel inlet is 13 m and 70 m respectively. At x = 13 m, during the initial developing phase, the development of roll wave shape is not totally accomplished, but apparent periodicity has appeared, and the flow depth is rather small, which is only 0.008 m; while at the distance of x = 70 m, the development of roll wave shape is fully completed, periodicity is even more apparent. The flow depth increases dramatically, up to 0.017 m, occurring in the final developing phase. From Figure 3, the three phases of the roll-wave development can be identified. As shown in Figure 4, the waveform experiences a clear periodic variation, which is very close to the experimental result of Brock (1969) as well as the numerical result of Zanuttigh and Lamberti (2002). Thus the accuracy of the present 1D model is further confirmed.

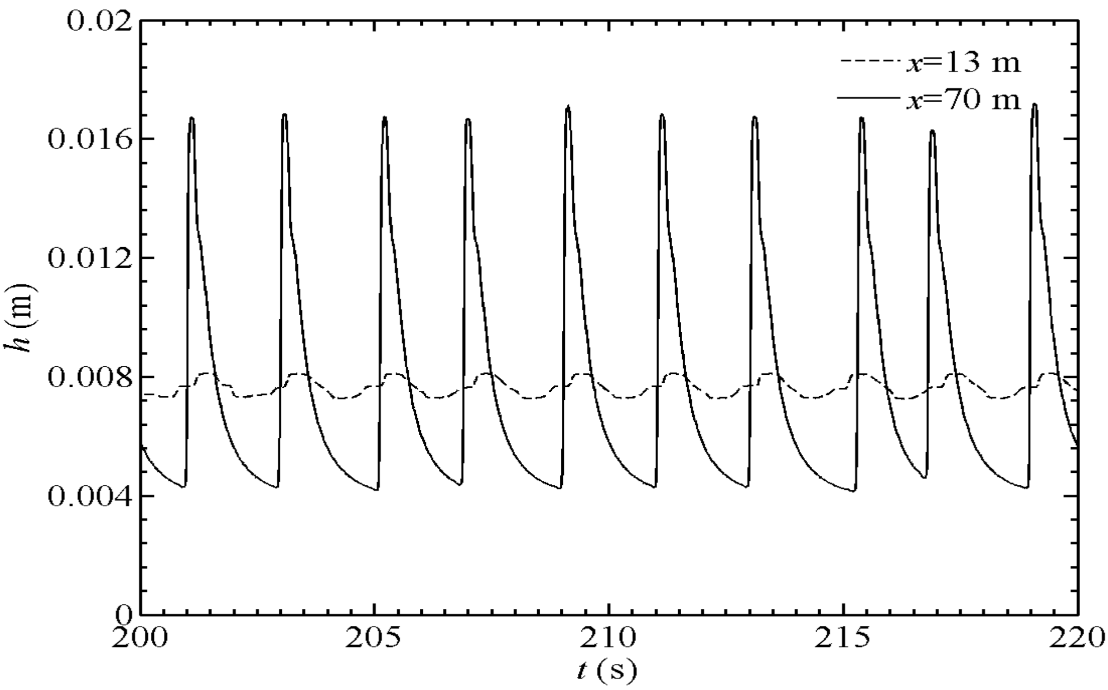

Figure 2. Water depth *h* versus time *t* at *x* = 13 m and 70 m from the channel inlet

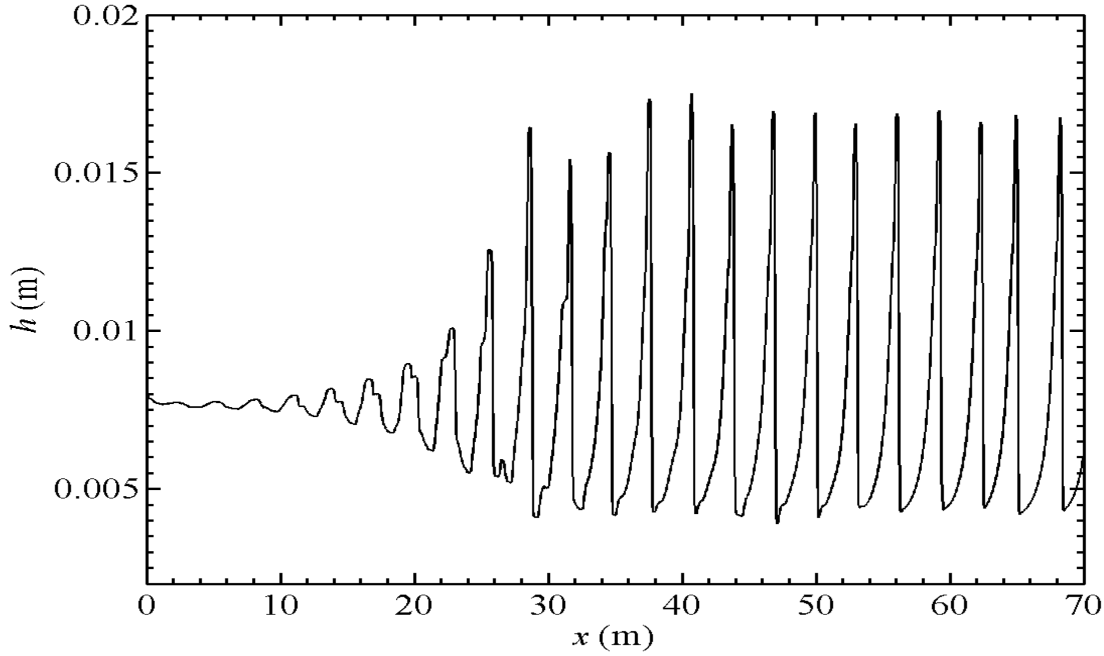

Figure 3. Profile of water depth

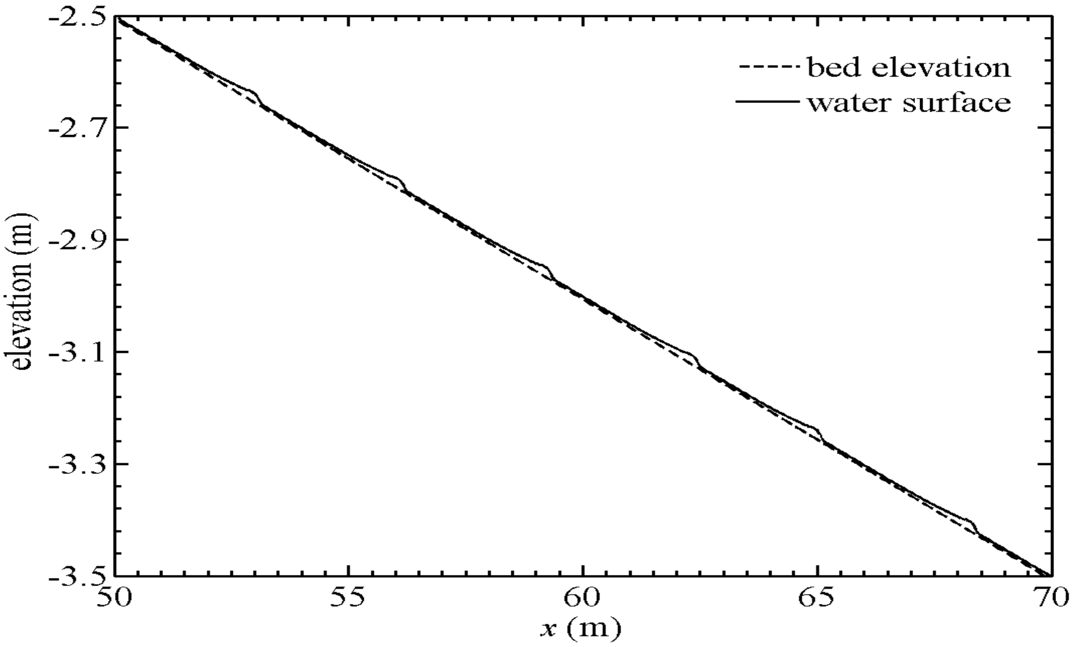

Figure 4. Water surface profile of roll waves

3.3 Role of surface tension

When the free surface is bending and the curvature radius is very small, the surface tension may be important. The spatially periodic structure of roll waves in shallow overland flows suggests that its impact needs to be clarified. For the analysis, a dimensionless parameter $\alpha = p_x / \tau$ is introduced, where $\tau = \rho g n^2 u^2 / h^{1/3}$ = bed shear stress. The ratio of the surface tension to bed shear stress is shown in Figure 5. It is shown that even in the fully developed phase of roll waves, when the surface tension reaches the maximum value, the order of magnitude of the ratio is only 10^{-3} and therefore surface tension is negligible as compared to bed shear stress.

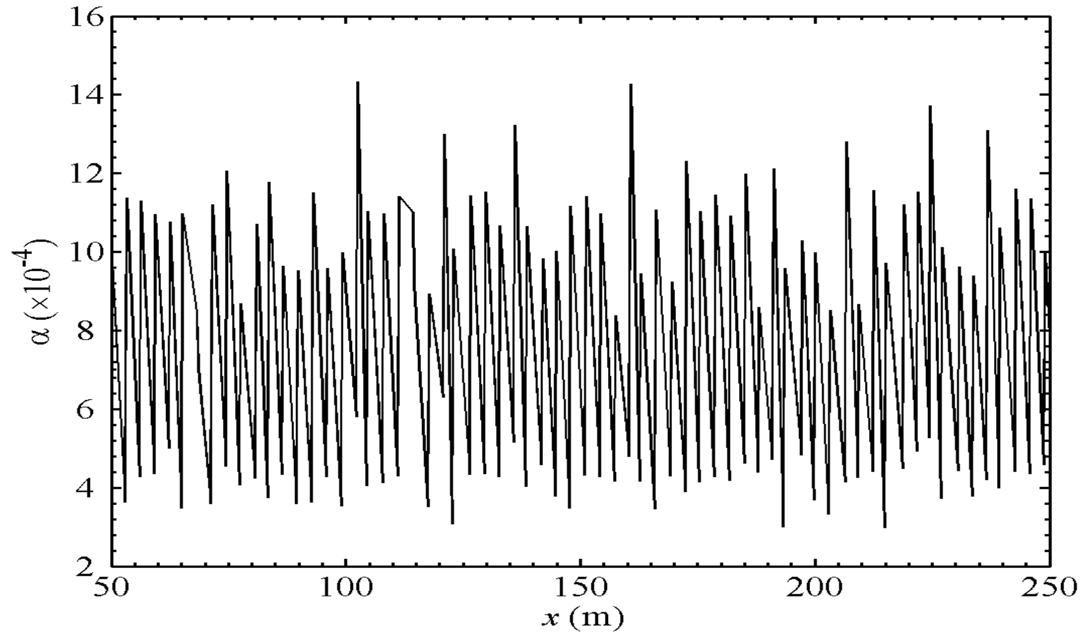

Figure 5. Ratio of surface tension to bed shear stress

4. ROLL WAVES OVER MOVABLE BED

4.1 Roll waves without infiltration

A comparison is presented to substantiate the difference of roll waves over erodible and fixed beds. The initial and boundary conditions over mobile bed are the same as over fixed bed, as described above.

The mechanism of sediment entrainment by overland flow has so far remained poorly understood, and inevitably its quantification bears much uncertainty. On this observation and also to avoid physically unrealistic large scour by overland flow, introducing the coefficient $\psi \ll 1$ to estimate sediment entrainment flux has been found to be essential. Here, a value of ψ =0.005 and 0.02 is considered respectively. The local variation of the deformation depth is shown in Figures 6a and 6b; while Figures 7a and 7b illustrate the variation of the corresponding flow depth. As is shown in Figures 6a and b, with the increase of the coefficient ψ, the entrainment flux E increases and the influence on bed deformation in the initial developing phase is greater, but in the final developing phase, the influence is less significant. Figure 6a shows the deformation depth in the initial developing phase of roll waves. It indicates that, when the coefficient ψ = 0.005, the deformation depth is minor, and the fluctuation of the bed is also small; when the coefficient ψ = 0.02, the deformation depth is relatively large, and so is the bed fluctuation. In Figure 6b, during the final developed phase of roll waves, when the coefficient ψ = 0.005, although the deformation depth is considerable, the fluctuation is relatively minor and the bed surface is relatively flat; when the coefficient ψ = 0.02, the deformation depth is considerable, and the deformation of bed surface shows great irregularity. Due to the complexity of the roll wave's hydraulic characteristics and the variation process of bed deformation, no definite corresponding relationship has yet been reported.

As is shown in Figure 7a, regardless of the pattern of the bed, the developing of roll waves have all experienced three phases, as were described by Brock. But for mobile bed, the amplification shows more disorder in the initial developing phase, the transition process is much longer, and the amplitude is more irregular than over the fixed bed.

In mobile bed, during the final developed phase of roll waves, as shown in Figure 7b, when the coefficient ψ = 0.05, despite that the deformation depth is considerable, the bed surface is relatively flat, the water depth profile of roll waves is very similar to that is over fixed bed. From 200 m to 220 m, both fixed bed and mobile bed have seventeen waves and the maximum water depth is 0.017 m. When the coefficient ψ = 0.2, the depth of deformation is much the same as it is when the coefficient ψ = 0.05, but the fluctuation of the bed surface is considerable, and notable variation occurs to the amplitude and waveform. There is a conspicuously difference between fixed bed and mobile bed. The number of waves decreases from seventeen to only five, while the maximum water depth increases from 0.017 m to 0.027 m.

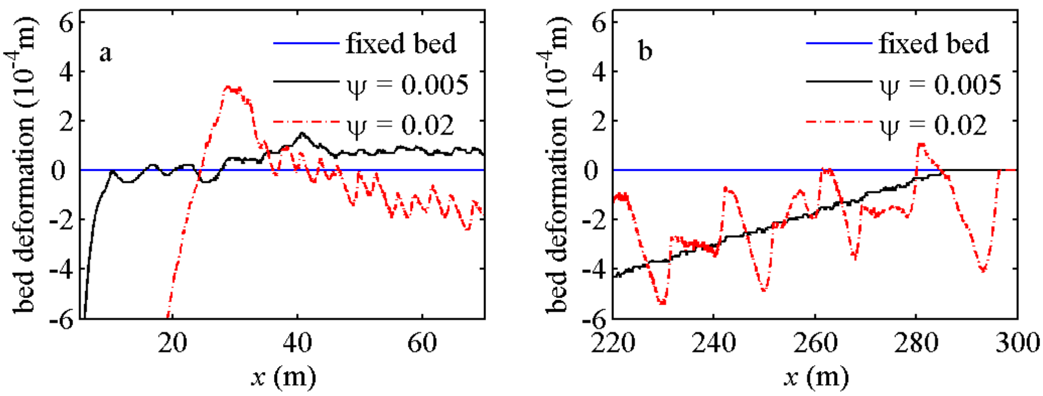

Figure 6. Profiles of bed deformation

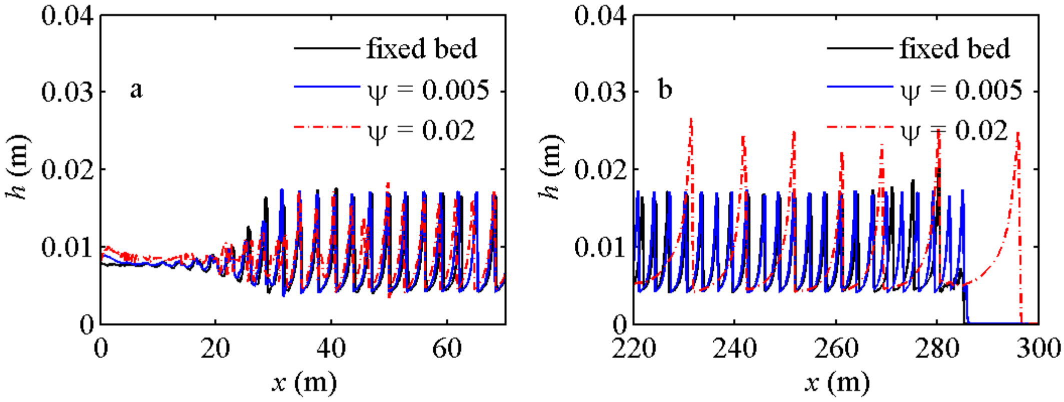

Figure 7. Profiles of water depth

As is shown in Figure 6a and Figure 7a, over mobile bed, during the initial developing phase and the overtaking phase, there is no significant corresponding relationship between the wave number, wave periodicity and the deformation depth. In the final developed phase, the deformation depth has little effect on the profiles of roll waves, and there is a good relationship between the bed deformation and the numbers of waves. The larger the coefficient ψ is, the greater the bed deformation is, and the bigger the growth of the volatility is. Meanwhile, the corresponding relationship between the bed deformation and the numbers of the waves is more apparent.

4.2 Roll waves with infiltration

The infiltration will have a certain effect on the roll waves in overland flow. The model calculates infiltration f by solving the original form of the Green-Ampt equation (Green and Ampt 1911):

$$f = K(1 + (\theta_s - \theta_i)B / N) \tag{9}$$

Where K = saturated hydraulic conductivity; B= Green-Ampt capillary head term; θ_s, θ_i = the saturated and initial volumetric water content, respectively (dimensionless); I = cumulative infiltrated depth.

As an example, ψ is set to be equal to 0.02 in comparison with the situation of no infiltration in Figure 8. Due to the infiltration, the roll waves have been attenuated, and the transmission distance has been shortened, but it has no significant effect on the periodicity of the roll waves.

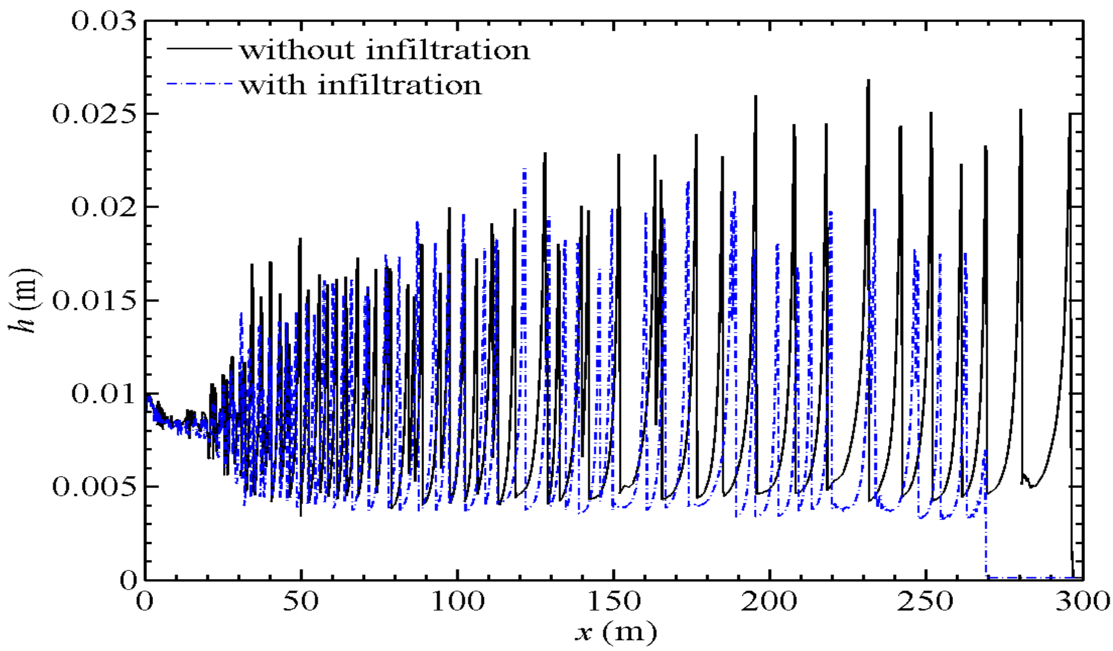

Figure 8. Water depth profile of roll waves with and without infiltration over the mobile bed

5. CONCLUSIONS

A 1D hydrodynamic model coupling flow, sediment transport and morphological evolution is slightly modified to investigate roll waves in overland flows over erodible bed. The model is first used to resolve roll waves as found in Brock's experiments (1969). Over fixed bed, the periodicity and the amplitude of the roll waves are very uniform and fixed. Over mobile bed, the roll waves are considerably altered as compared to their fixed-bed counterparts. The infiltration appears to result in attenuation of roll waves. The implication of the present finding is that incorporating sediment transport and morphological changes is critical in mathematical modeling of overland flows featuring roll waves in semi-arid and arid areas. This study is conceptual in nature. Enhancing the estimation of sediment entrainment by overland flow and extension to two dimensions will prove to be essential for practical applications.

ACKNOWLEDGEMENTS

The work reported in this manuscript is part of the research program funded by EU 6th Framework Program under project HYDRATE (Grant No. 037024) and also Natural Science Foundation of China (Grant No. 50739002).

REFERENCES

Balmforth, N.J., and Mandre, S. (2004), Dynamics of roll waves, Journal of Fluid Mechanics, 514, pp. 1-33.

Billett, S.J., and Toro, E.F. (1997), On WAF-type schemes for multidimensional hyperbolic conservation laws, *Journal of Computational Physics*, 130, pp. 1-24.

Brock, R.R. (1969), Development of roll wave trains in open channels, *Journal of Hydraulics Division*, ASCE, 95 (4), pp.1401-1425.

Cao, Z., Pender, G., Wallis, S., and Carling, P. (2004), Computational dam-break hydraulics over erodible sediment bed, *Journal of Hydraulic Engineering*, ASCE, 130, pp. 689-703.

Cornish, V. (1934), *Ocean waves and kindred geophysical phenomena*, Cambridge University Press, London.

Dressler, R. F. (1949), Mathematical solution of the problem of roll waves in inclined open channels, *Communications on Pure and Applied Mathematics*, 2, pp. 149 – 194.

Green, W.H., and Ampt G.A. (1911), Studies on soil physics, part 1-flow of air and water through soils, *Journal of Agricultural Sciences*, 4, pp. 1-24.

Liu, Q.Q., Chen L., Li, J. C., and Singh, V.P. (2005), Roll waves in overland flow, *Journal of Hydrologic Engineering*, ASCE, 10(2), pp. 110-117.

Richardson, J.F., Zaki, W. N. (1954), *Sedimentation and fluidization, part 1. Trans*, Inst. Chem. Engrg., 32, pp. 35–53.

Sander, G. C., Parlange, J. Y., Barry, D. A., Parlange, M. B., and Hogarth, W. L. (2007), Limitation of the transport capacity approach in sediment transport modeling, *Water Resources Research*, 43, doi: 10.1029/2006WR005177.

Toro, E.F. (2001), *Shock-Capturing Methods for Free-Surface Shallow Flows*, Wiley, Chichester, England.

Thomas, H.A. (1937), *The Propagation of stable wave configurations in steep channels*, Carnegie Institute of Technology, Pittsburgh.

Zanuttigh, B., and Lamberti, A. (2002), Roll waves simulation using shallow water equations and Weighted Average Flux method, *Journal of Hydraulic Research*, IAHR, 40(5), pp. 610-621.